

VSP-CDP TRANSFORM IN ANISOTROPIC MEDIA

César P. Vásquez and Reinaldo J. Michelena, Intevep, S.A., Venezuela

SUMMARY

VSP reflection imaging techniques require accurate velocity models to effectively image the data. VSP to CDP transform is usually applied in media described by homogeneous isotropic flat layers. In the presence of transversely isotropic layers (shales for example) or in the presence of fractures, isotropic velocity models may be inadequate and reflections events may be positioned incorrectly. We propose a VSP to CDP transform algorithm that treats properly the anisotropy of the medium and positions events in their proper reflection place. The algorithm, conceptually similar to the conventional ones, is based on anisotropic ray tracing in heterogeneous models described by a set of homogeneous layers. The anisotropic parameters (elastic constants) that described such models can be estimated tomographically. By using anisotropic ray tracing, we calculate the reflections points and the traveltimes of the corresponding events. Using these positions and traveltimes, reflection data in the (t,z) domain are transformed into data in the (x,z) domain, yielding an image of the medium of interest.

Synthetic examples show that the anisotropy effects increases with the angle of incidence when transforming P wave data generated in transversely isotropic media. This effect can be non-negligible when the shallow strata are anisotropic or when the source-well separation is comparable or greater than the depth of the target. By using our algorithm, the effect of the anisotropic layers is alleviated, yielding a more reliable image of the zone of interest.

INTRODUCTION

The effect of anisotropy in seismic wave propagation has been well established and associated mainly with the presence of shales, fractures, differential stresses, and fine layering effects. Both P wave anisotropy, where velocity varies with direction of propagation, and S wave anisotropy, where velocity varies with direction of propagation and polarization angle, have been observed in actual fields experiments (Bamford and Nunn, 1979; Crampin et al., 1980; Johnston, 1986; Lynn, and Thomsen, 1990), laboratory studies (Lo, et al., 1986; Rai and Hanson, 1988), and in physical model studies (Melia and

Carlson, 1984).

Depending on the degree of anisotropy, seismic sections obtained under isotropic assumptions may be significantly distorted since reflection events can be mispositioned both laterally and vertically. Vertical misposition of events in seismic section from surface geometries have been reported (Banik, 1984) and well studied (Alkhalifah and Lerner, 1994; Lerner and Cohen, 1993). For crosswell geometries, anisotropy can cause severe distortions in velocity tomograms obtained under the assumption of isotropic velocities (Carrion et al., 1992; McCann et al., 1989). Moreover, reflection images obtained using these distorted tomograms will also be in error. However, as far as we know, these errors haven't been quantified for neither VSP nor crosswell geometries, and the current algorithms used to obtain reflection images from these type of data (Wyatt and Wyatt, 1984; Lazaratos et al., 1993; Mo and Harris, 1993) do not take into account the effects of velocity anisotropy.

In this paper we propose an algorithm to obtain reflection images from either VSP or crosswell data using anisotropic velocities. The algorithm we propose is a variation of the VSP-CDP transform introduced by Wyatt and Wyatt (1984). The main difference between our algorithm and Wyatt and Wyatt's is that in ours reflection traveltimes are calculated by ray tracing in anisotropic media. We obtained that the errors introduced by anisotropy increase with angle of incidence and, in some situations, anisotropy can introduce event mispositions of the order of a wavelength. Our algorithm corrected these effects in the synthetic example studied.

In this study we do not deal with the problem of estimating anisotropic velocities. Since we focused at this point in synthetic data, we used for the transformation the same velocity model used to generate the data. When applying the algorithm to field data, the anisotropic velocity model will be estimated using anisotropic traveltime tomography (Michelena et al., 1995).

ANISOTROPIC VSP-CDP ALGORITHM

In this section, we briefly describe the algorithm we are proposing to do VSP-CDP transformation in anisotropic

media. This algorithm is a variation of the VSP-CDP transform originally proposed by Wyatt and Wyatt (1984) and implemented for cross-well geometries by Lazaratos et al. (1993). All these algorithms map each data point to a possible reflection point inside the model by means of ray tracing in a given isotropic velocity model.

When the medium is isotropic, the velocities can be estimated from the sonic logs or by inverting the first arriving downgoing waves. When the medium is anisotropic, the sonic velocities are no longer good estimates of medium velocities since sonic logs only sample the vertical component of the velocity. These difficulties can be overcome by estimating the velocities in anisotropic models from the first arriving energy, by means of traveltimes tomography, as described by Michelena et al. (1995).

Once the anisotropic velocities are estimated, we need to trace rays in anisotropic media to calculate the reflection points where the data are going to be mapped. In this paper, we use a ray tracing algorithm originally proposed by Byun (1984).

The mapping algorithm consists of four basic steps: (a) Generation of traveltimes maps from source/receivers positions to all points in the model. (b) Generation of migration ellipses by summing the time maps corresponding to all source/receiver pairs. Each ellipse define, for a given time, the positions of all possible virtual reflections inside the model. (c) Calculation of trajectories connecting all possible reflection points from all depths for each source-receiver pair. The calculation of the trajectories is made by applying the Fermat's principle to the migration ellipses calculated in step (b). The traveltimes associated with each reflection point are also saved in this step. There is a trajectory for each source-receiver pair. The seismic trace that corresponds to each source-receiver pair will be mapped along its corresponding trajectory. (d) Data mapping from the original (z,t) domain to the (z,x) image domain. The amplitudes from the traces are mapped along the corresponding trajectories using the traveltimes calculated in (c).

The algorithm just described assumes the data contains only a single reflected wave type. Since VSP data contain a rich variety of wave types (downgoing P, P-P reflections, P-S reflections, S-S reflections, P-S transmissions, etc.), it is mandatory to extract the desired reflection mode by filtering out the rest. As we show in the next section, the Radon transform is a good tool to achieve such a goal.

SLANT STACK WAVEFIELD SEPARATION

The slant stack transformation consists of summing the amplitudes of the given data set in the $(\text{space}, \text{time})$ domain along slanted straight lines with a given slope p and intercept time τ . The result of the sum is assigned to the corresponding point in the (τ, p) domain and the process is repeated again for all slopes and all intercepts. A basic property of this transformation is that straight lines in the space-time domain are transformed into points in the (τ, p) domain, and vice versa. In the absence of strong lateral velocity variations, reflections in VSP data are either linear or piece wise linear, which means that after slant stack they should transform into points or well localized regions in the (τ, p) domain (assuming wide aperture data). Since downgoing events, P-P reflections, P-S reflections and S-S reflections have different slopes and intercept times, they transform into separate regions in the (τ, p) domain and therefore, they should be easy to separate.

To test these ideas, we generated synthetic data using the model shown in Figure 1. This Figure also shows the VSP array used to generate the data. The model consist of four layers, three isotropic and one anisotropic. The anisotropic layer is located between 2000 and 3000 ft. The magnitude of the anisotropy is 20% (elliptical).

We used finite differences in anisotropic media to generate the synthetic data (from explosive source) used to test the algorithm. Figure 2 shows all the different wave-modes generated after a downgoing P-wave impinges upon the different interfaces. The image is clipped to enhance the reflections, which are much weaker in reality than the downgoing P-wave.

In this example, we'll concentrate on mapping P-P upcoming reflections. That's why before the mapping, we need to separate and enhance these reflections from the rest of the wavefield. Figure 3 shows how the data set of Figure 2 looks like in the (τ, p) domain. By examining the slopes (p) and intercepts (τ) of the different events in the original data, we can identify them in the transformed domain. Only downgoing events have positive p , which means they can be filtered out by simply removing positive p in the (τ, p) domain. Both slope and intercept for S-waves are different than slope and intercept for P-waves, which explains, as we will see next, why they are well separated in the (τ, p) domain.

Figure 4a shows the data in the (τ, p) domain after filtering

downgoing events (positive p) and upcoming P-S reflections. The filter we used has a sin-like taper to minimize edge effects, and it acted only on the ray parameter axis. Figure 4b shows the data back to the VSP domain after filtering in (τ, p) and applying a transpose slant stack operation. Primary upcoming P-P reflections were enhanced, but other upcoming converted P-wave modes are still present in the data because we performed the filtering based on slopes only.

VSP-CDP IMAGING

In this section we compare the results of transforming the data of Figure 4b with both isotropic and anisotropic VSP-CDP transform algorithms. Two velocity models were used. For the isotropic case, we use an isotropic velocity model created by using the vertical velocities of the original model (Figure 1). By using this type of model we wanted to simulate the usual practice of estimating the medium velocities from the sonic (vertical) velocities. For the anisotropic case, we used the original anisotropic velocity model.

Figure 5a shows the result of the VSP-CDP transformation when using a isotropic velocity model. The event at 2000 ft has been positioned correctly because velocities in the upper layer are isotropic. The event at 3000 ft, at the bottom of the anisotropic layer, has been mispositioned. The error in the location of the event increases with the angle of incidence (as the event gets closer to the well), which can be explained by the increase of velocity with angle in the original anisotropic model that was not taken into account when using the isotropic algorithm. The event at 4000 ft is also mispositioned. In this case, the error is approximately constant with horizontal distance (unlike the event at 3000 ft) because the angle of incidence doesn't change significantly at this greater depth.

Figure 5b shows the result of the VSP-CDP transformation when using the anisotropic algorithm. All events are positioned correctly because the velocity anisotropy has been taken into account. Small artifacts along the events are produced by inaccuracies in the ray tracing algorithm.

Since velocity increases with angle of incidence in this example, the interval times calculated between reflections at two different depths decrease, introducing significant stretching of the wavelet. Interpreters not familiar with this effect may observe reflector dips which don't exist in reality. To correct this effect, we did a time shift to the original data equal to half a period. This shift simulates quasizero-phase data.

CONCLUSIONS

We have implemented an algorithm for anisotropic VSP-CDP transformation that positions events in their correct position regardless of the magnitude of the anisotropy. This algorithm is a generalization of the conventional ones, the new ingredient being the traveltimes calculations performed in anisotropic media. With synthetic examples, we showed the effects of the anisotropy in conventional VSP-CDP transform. The events are mispositioned, and this error increases with increasing incidence angle. We also showed with synthetic examples that the slant stack wave field separation is a robust tool to separate and enhance P-P reflections from the rest of the total wave field. In our examples, we use the same velocity model used to generate and to transform back the synthetic data. With field data, the estimation of velocities can be done with anisotropic traveltimes tomography.

REFERENCES

- Bamford, D. y Nunn, K. R., 1979, In_Situ seismic measurements of crack anisotropy in the carboniferous limestone of northwest England: *Geophys. Prosp.*, 27, 322-338.
- Banik, N. C., 1984, Velocity anisotropy of shales and depth estimation in the North Sea basin: *Geophysics*, 49, 1411-1419.
- Byun, B. S., 1984, Seismic parameters for transverseley isotropy media: *Geophysics*, 49, 1908-1926.
- Byun, B. S., Corrigan, D, and Gaiser, J. E., 1989, Anisotropy velocity analysis for lithology discrimination: *Geophysics*, 54, 1564-1574.
- Crampin, S., Mc Gonigle, R., and Bamford, C., 1980, Estimating crack parameters from observations of P-wave velocity anisotropy: *Geophysics*, 45, 345-360.
- Lazaratos, S. K., Rector, J. W., Harris, J. M. y Schaack, M. V., 1993, High-resolution, cross-well reflection imaging: Potential and technical difficulties: *Geophysics*, 58, 1270-1280.
- Lo, T. W., Croyner, K. B., and Toksoz, M. N., 1986, Experimental determinations of elastic anisotropy of Berea sandstone, Chicopee shale and Chelmsford granite: *Geophysics*, 51, 164-171.
- Lynn, H. B., and Thomsen, L. A., 1990, Reflections shear-wave collected near the principal axes of aximuthal anisotropy: *Geophysics*, 55, 147-156.
- Melia, P. J, and Carlson R. L., 1984, An experimental test of P-wave anisotropy in stratified media: *Geophysics*, 49, 374-378.
- Michelena, R. J., Muir, F, and Harris, J. M., 1995, Crosswell tomographic estimation of elastic constants in heterogeneous

transversely isotropic media: Geophysics, in press.

Rai, C. S, and Hanson, K. E., 1988, Shear-wave velocity anisotropy in sedimentary rocks: A laboratory study: Geophysics, 53, 800-806.

Wyatt, K. D, and Wyatt, S. B., 1984, Determining subsurface structure using the vertical seismic profiling: in Toksoz, M. N. y Stewart, R. R., Eds., Vertical Seismic Profiling: Advance Concepts, Geophysical Press.

Thanks to Intevp, S.A. for permission to publish this work.

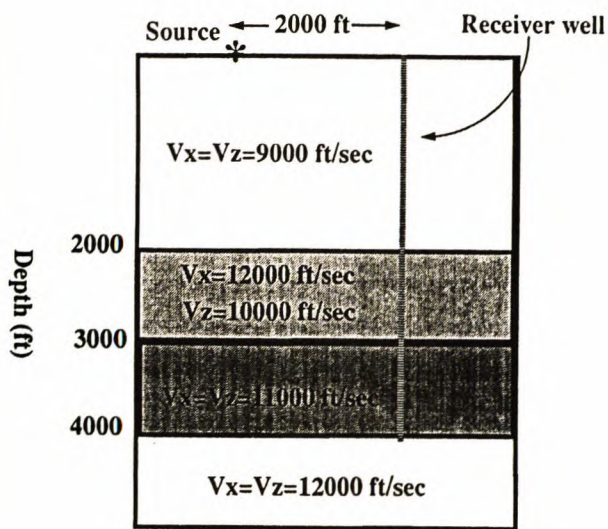


Fig. 1. Anisotropic velocity model and the VSP array used to generate synthetic data.

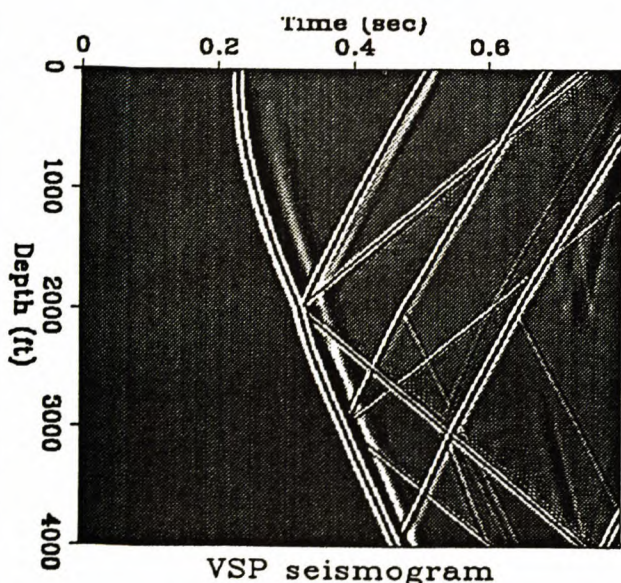


Fig. 2. VSP synthetic seismogram.

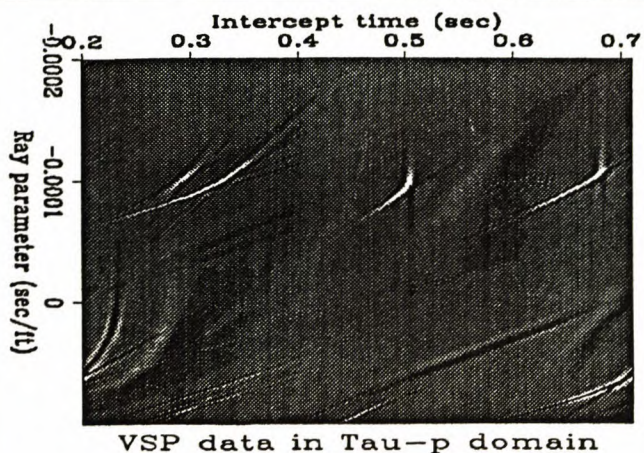


Fig. 3. VSP data in Tau-p domain.

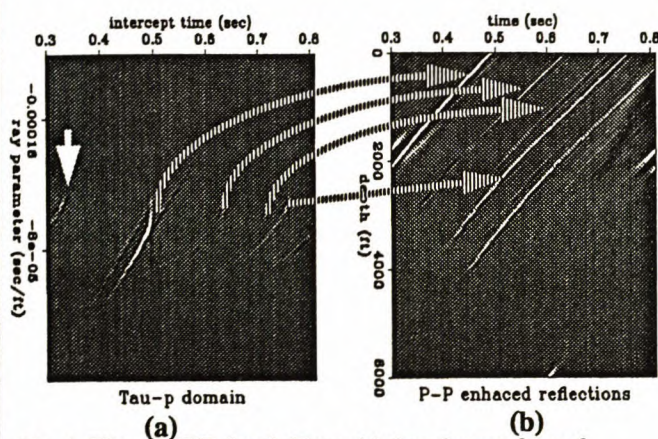


Fig. 4. Filtered VSP data in Tau-p (a) domain transformed into upcoming P waves (b).

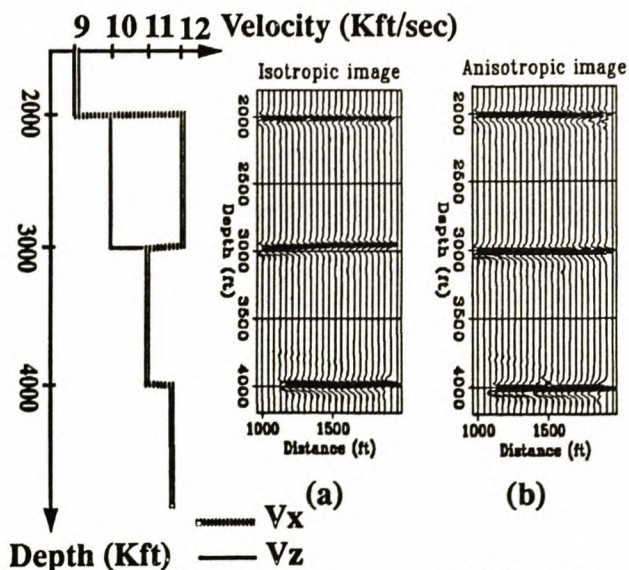


Fig. 5. The figure shows images of model of Fig. 1. (a) Using a conventional VSP-CDP algorithm. (b) Using the anisotropic VSP-CDP transformed.